Journal of Organometallic Chemistry 952 (2021) 122025

Contents lists available at ScienceDirect

Journal of Organometallic Chemistry

journal homepage: www.elsevier.com/locate/jorganchem

Pd nanoparticles supported on pyrazolone-functionalized hollow mesoporous silica as an excellent heterogeneous nanocatalyst for the selective oxidation of benzyl alcohol

Somayeh Ghorbani, Rouhallah Parnian, Ebrahim Soleimani*

Department of Organic Chemistry, Faculty of Chemistry, Razi University, Kermanshah 67149-67346, Iran

ARTICLE INFO

Article history:
Received 5 June 2021
Revised 3 August 2021
Accepted 11 August 2021
Available online 15 August 2021

Keywords:
Hollow mesoporous silica
Palladium NPs
Selective oxidation of benzyl alcohols
pyrazolone-based ligand

ABSTRACT

Hollow mesoporous silica nanoparticles (HMSNs), by exploiting both their organo-functionalized surface and porous shell were chosen as the ideal support for the immobilization of palladium nanoparticles (Pd-NPs). The HMSNs were created by acidic removal of Fe_3O_4 nanoparticles from silica-coated Fe_3O_4 core-shell. The catalyst was prepared following surface modification of HMSNs by (3-chloropropyl)-triethoxysilane (CPTES), functionalization by pyrazolone-based ligand, and stabilization of Pd-NPs on HMSNs. The resulting catalyst was fully characterized by different analytical techniques. This new heterogeneous catalyst showed high catalytic activity and excellent selectivity in the selective oxidation of benzyl alcohols in ethanol at ambient temperature. Easy separation by centrifuge and reusability for five successive cycles without significant loss of catalytic activity were some advantages of this catalyst.

© 2021 Elsevier B.V. All rights reserved.

1. Introduction

Recently, heterogeneous supported catalyst systems, due to their potential applications for replacing homogenous catalysts, have made great progress in organic chemistry and industry; they exhibit many advantages such as easy separation from the reaction medium, stability, their available active sites, reusability, simplified recovery, green chemical processes, and enhanced product selectivity, which are all important factors in organic chemistry and industry [1–4]. Supported catalysts on solid materials are available in different types such as carbon, zeolites, hydroxyapatite, silica, and organic polymers; however, silica-based materials have received much attention, due to their special properties of excellent stability (chemical and thermal), no swelling, facile and low-cost synthesis, high surface area, good accessibility, and easy surface modification to provide catalytic center [5–8]. Among various types of silica materials, hollow mesoporous silica nanoparticles (HMSNs) with hollow interior spaces have demonstrated promising applications in various fields, such as catalysts, supports, nanoreactors, drug delivery, photonics, biotechnology, and electrochemical cells [9–14]. This is due to their unique properties, including hollow interior space, penetrating mesoporous shell, high specific surface area, low density, stability, and good biocompatibility [15–17]. The presence of an interior void space makes HMSNs unique nanoreactors to load active species for catalytic reactions. HMSNs have also shown more storage capacity in drug delivery applications compared to conventional mesoporous silica NPs [18], Furthermore, owing to the mesoporous shell, the transport of guest molecules (dyes, drugs, catalysts, etc.) into and out of the hollow void spaces is possible [19,20]. Beside, different organic, inorganic, or organometallic groups can modify the mesoporous shell of HMSNs to provide a catalytic center [21,22].

The selective oxidation of benzyl alcohols is one of the essential organic transformation reactions in academic research and industrial production [23–25]. Many catalyst systems have been developed for the selective oxidation of benzyl alcohols. However, benzyl alcohols have been traditionally oxidized by stoichiometric amounts of toxic and expensive oxidants, such as potassium permanganate, potassium dichromate, sodium hypochlorite, and organic peroxides [26,27]. Thus, many studies on mild oxidation methods of alcohols with less toxic reagents have been carried out extensively to develop environmentally benign oxidation systems [28–31]. In this regard, a wide variety of heterogeneous catalysts have been created. Among the reported catalysts, supported transition metal nanoparticles (e.g., Pt, Pd, Ru, and Au NPs) have been extensively investigated in the selective oxidation of alcohols [32–43]. In particular, supported Pd-NPs have attracted extensive interest because of their advantages, such as excellent activity and selectivity, recyclability, environmental issues, and economic aspects [44–54]. Ideally, excellent support in metal NPs-based catalysts should have a functionalized surface to good dispersion of

* Corresponding author.
E-mail address: e_soleimanirazi@yahoo.com (E. Soleimani).

https://doi.org/10.1016/j.jorganchem.2021.122025
0022-328X/© 2021 Elsevier B.V. All rights reserved.

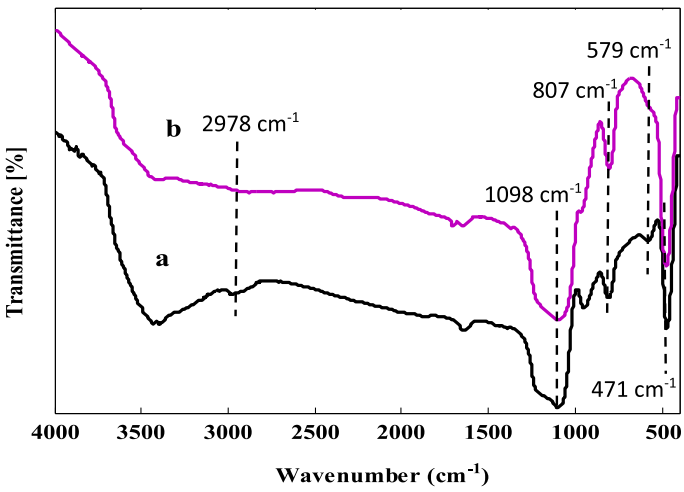

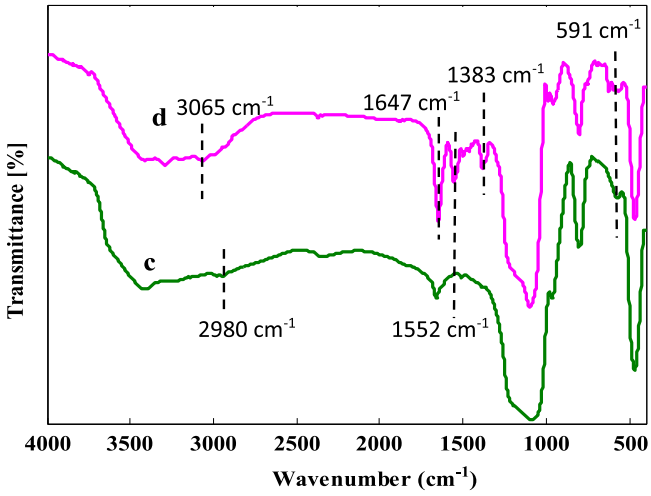

Scheme 1. Selective oxidation of benzyl alcohols.

metal NPs, a large surface area for high accessibility of active sites, a hollow construction to facile mass transportation, and a porous structure to anchor the metal NPs [55]. More recently, HMSNs as an ideal support to immobilize the Pd-NPs have attracted considerable attention for the selective oxidation of alcohols [56–62].

Pyrazolone derivatives, as an important class of organic compounds, have significant applications in medicinal chemistry, catalysis, dye, analytical purposes, and extraction of different metal ions [63–68]. Owing to their electron-rich donor sites, pyrazolone derivatives have been extensively used as chelating ligands to form various types of metal complexes [69,70]. Many of these metal complexes have potential biological applications as anticancer [71,72] or antimicrobial agents [73,74]. They have also been used as an appropriate catalyst in organic transformations [75–77]. Accordingly, for the first time, we here use a bis-pyrazolone-based ligand, 4,4′-((4-hydroxyphenyl)methylene)bis(3-methyl-1H-pyrazol-5-ol) (denoted as Pyra), for the immobilization of Pd-NPs on heterogeneous nanocatalyst.

Based on the mentioned background, we present an efficient route for the synthesis of novel Pd-NPs supported on functionalized hollow mesoporous silica NPs, which afford high performance as a heterogeneous catalyst. The HMSNs were prepared through the hard template approach using magnetite nanoparticles as a hard appropriate template, which can be easily removed by acid treatment. Then, functionalization of HMSNs was performed using bis-pyrazolone-based chelating ligand, 4,4′-((4-hydroxyphenyl)methylene)bis(3-methyl-1H-pyrazol-5-ol). The mesoporous silica shell provides organo-functionalized support for the immobilization of Pd-NPs. It also stabilizes the Pd-NPs on its pores to enhance catalytic activity. For heterogeneous catalysis, this novel catalyst displayed excellent selectivity and activity for the oxidation of benzyl alcohols using hydrogen peroxide as an oxidant (Scheme 1).

2. Results and discussion

2.1. Catalyst characterization

Silica-coated magnetic nanoparticles were used for the synthesis of HMSNs. The detailed structure and step-by-step synthetic procedures of Pd-NPs supported on functionalized HMSNs (denoted as Pd/HMSNs∼Pyra/Pd) are depicted in Scheme 2. Initially, Fe_3O_4 NPs as hard template was prepared according to the reported method (co-precipitation) [78]. Following the sol-gel procedure [79], a mesoporous silica shell was coated on the surface of Fe_3O_4 NPs using tetraethyl orthosilicate (TEOS) and cetyltrimethylammonium bromide (CTAB) as a source for the formation of mesopores. To obtain the HMSNs, ethanolic HCl solution was used as a useful etching reagent to completely etch both of Fe_3O_4 NPs and CTAB templates from the Fe_3O_4@CTAB/SiO_2 core-shell in a single step. Then, for the surface functionalization of HMSNs with organic moiety, the surface was first modified using 3-chloropropyltriethoxysilane (CPTES) as a linker between the organic moiety and the support. 4,4′-((4-hydroxyphenyl)methylene)bis(3-methyl-1H-pyrazol-5-ol) as a ligand was prepared according to our reported method [80], and then connected to the immobilized HMSNs. Finally, Pd/HMSNs∼Pyra/Pd nanocatalyst was prepared by adding $Pd(OAc)_2$ and then using $NaBH_4$ as a reducing agent to synthesize and stabilize Pd-NPs on both pyrazolone-based ligand and porous shell.

The prepared catalyst was comprehensively analyzed by various techniques, such as transmission electron microscopy (TEM), scanning electron microscopy (SEM), Fourier transform infrared spectroscopy (FT-IR), X-ray powder diffraction (XRD), dispersive X-ray spectroscopy (EDX), thermogravimetric analysis (TGA), inductively coupled plasma (ICP) and BET.

FT-IR analysis was used to ensure the presence of new functional groups, and to investigate the removal of CTAB and Fe_3O_4 NPs templates. Fig. 1a shows the FT-IR spectrum of Fe_3O_4@CTAB/SiO_2 NPs and their band characteristics. The signal attributed to the Fe-O bond vibration is observed at 579 cm^{-1}. A strong broad peak around 1098 cm^{-1} arises from the Si-O-Si asymmetric stretching vibrations. The bands at 807 cm^{-1} and 471 cm^{-1} correspond to the Si–O symmetrical stretching vibration [81,82], that indicated the existence of a SiO_2 layer [83]. Furthermore, the peaks appearing at 3200–3500 cm^{-1} and 1633 cm^{-1} are attributed to the O–H stretching and H–O–H bending vibrations of surficial hydroxyl groups and adsorbed water, respectively [84]. The C-H stretching vibrations, which can be seen at 2978 cm^{-1} are due to the CTAB template. Comparing Fig. 1a with Fig. 1b, after removing the templates in acidic solution, the C-H stretching vibrations at 2978 cm^{-1} and the Fe-O bond vibration at 579 cm^{-1} disappeared, which confirmed the removal of both CTAB and Fe_3O_4 NPs templates and creation of HMSNs (Fig. 1b). In the case of HMSNs∼Cl, the peaks at 2980 cm^{-1} and 591 cm^{-1} correspond to stretching vibrations of C–H and C-Cl bonds of CPTES, respectively (Fig. 1c). The FT-IR spectrum of 4,4′-((4-hydroxyphenyl)methylene)bis(3-methyl-1H-pyrazol-5-ol) (Pyra) includes the O-H stretching vibration at 3403 cm^{-1}, CH_3 bending vibration at 1380 cm^{-1}, and aromatic C=C stretching vibration at 1595 cm^{-1} and 1483 cm^{-1} [80]. In

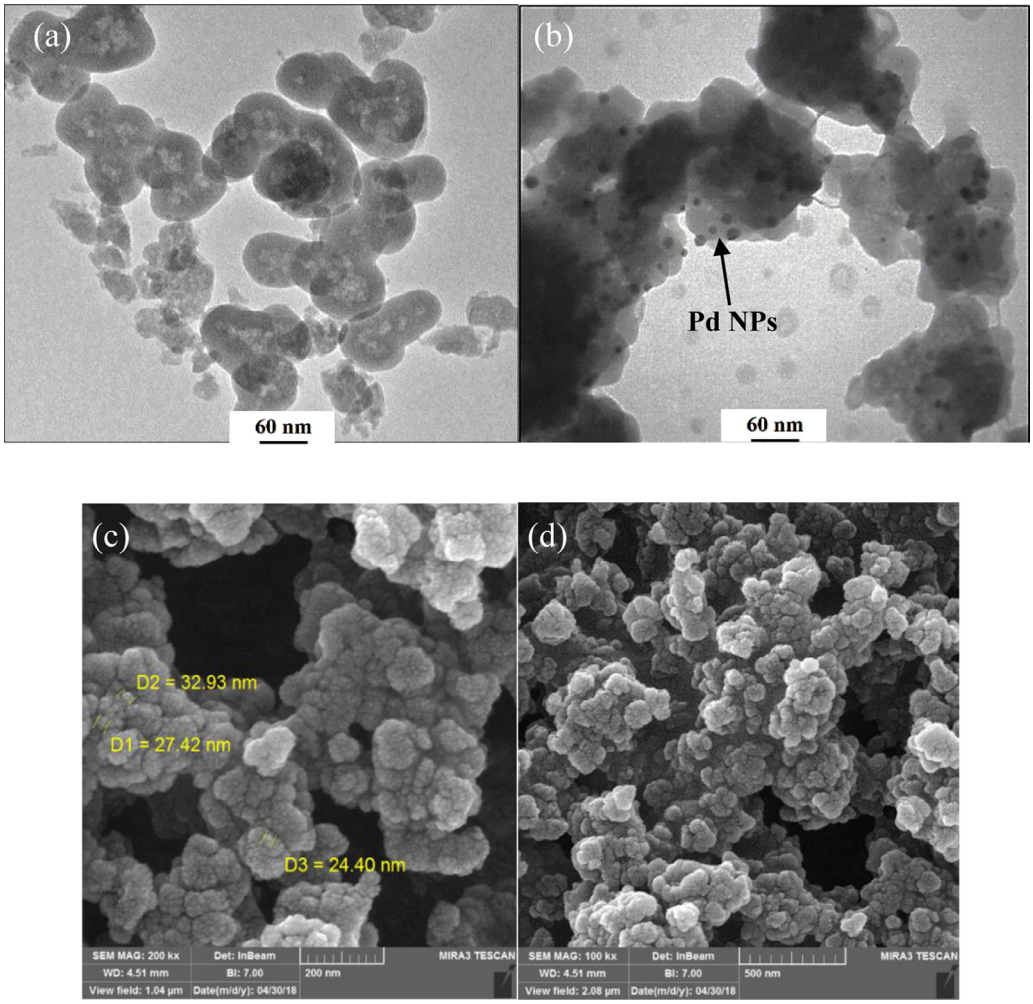

Scheme 2. The step-by-step synthetic procedures of Pd/HMSNs~Pyra/Pd catalyst.

Fig. 1d, aromatic C=C stretching vibration at 1647 cm^{-1} and 1552 cm^{-1}, CH_3 bending vibration at 1383 cm^{-1}, and the C-H stretching vibration of the phenyl group at 3065 cm^{-1} confirmed the presence of pyrazolone-based ligand on the surface of HMSNs.

The morphology of the catalyst was observed by transmission electron microscopy (TEM) (Fig. 2a and b). The TEM images of HMSNs (Fig. 2a) clearly show the central hollow cores generated by removing Fe_3O_4 NPs. All the hollow silica nanoparticles are well dispersed, separated from each other, and with well-defined morphology. The average size of the cores was found to be ~20–30 nm. The thickness of the silica shell was around 15–20 nm. In Fig. 2b, it can be seen that Pd-NPs with a size of ~5–8 nm have been immobilized on the HMSNs. The average size of Pd-NPs is consistent with the crystallite size of 5.6 nm for Pd obtained from the XRD results. The SEM images in Fig. 2c show the granular and spherical morphology for Pd/HMSNs~Pyra/Pd NPs with an average size of ~25–35 nm, which is consistent with the TEM results.

Powder XRD diffraction pattern (Fig. 3) obtained for the Pd/HMSNs~Pyra/Pd catalyst exhibited a broad reflection at $2\theta = 22.9°$ corresponding to the amorphous silica support. Three additional reflections at $2\theta = 39.81°$, 46.05°, 67.50°, corresponding to the (111), (200), (220) lattice planes, confirmed the formation of a metallic face-centered cubic (fcc) Pd crystal structure [85,86]. The crystallite size of Pd was calculated from the Scherrer formula and found to be an average diameter of 5.6 nm.

The elemental analysis of the nanocatalyst was determined by the EDX technique. The EDX spectrum in Fig. 4 shows the presence of C, N, Si, O, and Pd in the structure of Pd/HMSNs~Pyra/Pd nanocatalyst. Therefore, successful functionalization of HMSNs can be inferred from this technique.

Beside, the surface area and porosity of the HMSNs~Pyra and Pd/HMSNs~Pyra/Pd nanocatalyst were characterized. The N_2 adsorption-desorption isotherms of HMSNs~Pyra and Pd/HMSNs~Pyra/Pd are shown in Fig. 5. The isotherms are Type IV, which is typical for mesoporous materials, and the isotherm of nanocatalyst (Pd/HMSNs~Pyra/Pd) indicate that palladium introduction doesn't affect the mesoporous structure of the HMSNs; however, surface area decreases from 87/48 to 76.36 m^2g^{-1} for HMSNs~Pyra and Pd/HMSNs~Pyra/Pd respectively. The loading of palladium nanoparticles on the external surface or in the pore channels of HMSNs may block nitrogen flow into the pores, leading to the decrease of specific surface area. Barrett-Joyner-Halenda (BJH) pore size distribution analysis showed a pore diameter of 4.4 nm for HMSNs~Pyra and 1.2 nm for Pd/HMSNs~Pyra/Pd.

Thermogravimetric analysis (TGA) was used to demonstrate the amount of organic moiety in the nanocatalyst and exhibit the thermal stability of the HMSNs. TGA curves of HMSNs~Cl and HMSNs~Pyra are presented in Fig. 6. The initial weight loss observed below 200 °C is related to the adsorbed moisture in the samples. The TGA curves show decomposition temperature started

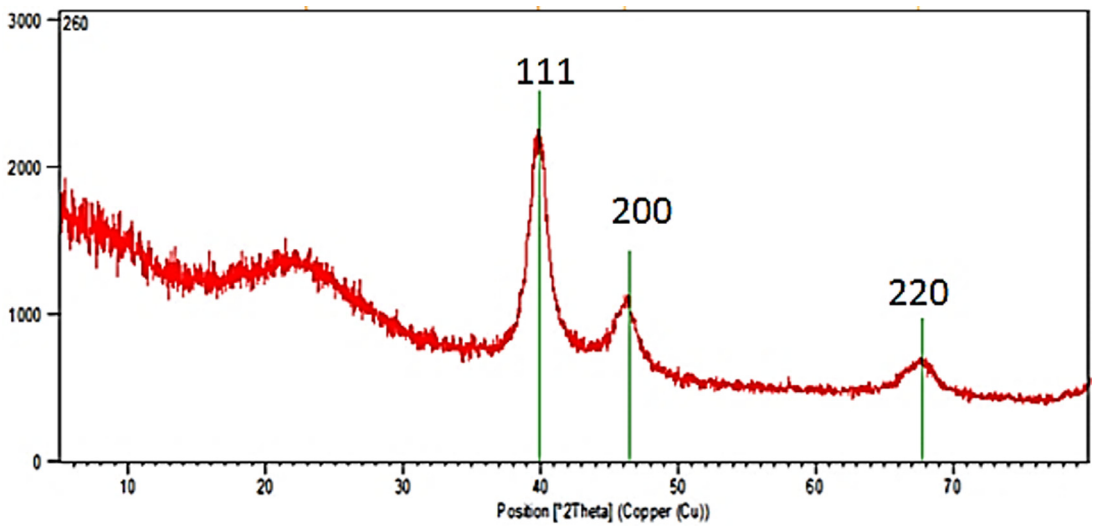

Fig. 1. FT-IR spectra of (a) Fe_3O_4@CTAB/SiO_2, (b) HMSNs, (c) HMSNs~Cl and (d) HMSNs~Pyra.

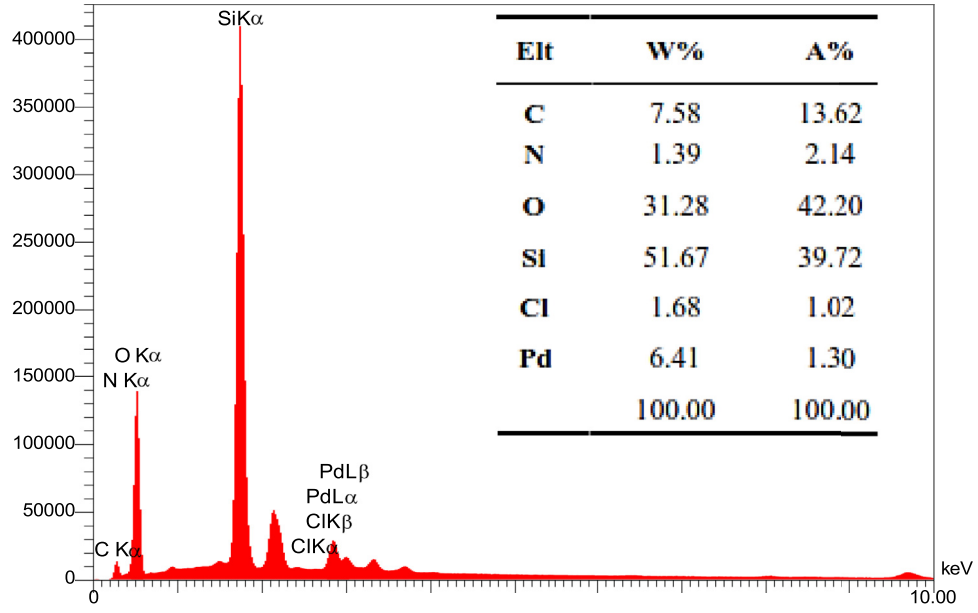

Elt	W%	A%
C	7.58	13.62
N	1.39	2.14
O	31.28	42.20
Si	51.67	39.72
Cl	1.68	1.02
Pd	6.41	1.30
	100.00	100.00

Fig. 2. TEM images of HMSNs (a) and Pd/HMSNs~Pyra/Pd (b), SEM images of Pd/HMSNs~Pyra/Pd (c) and (d).

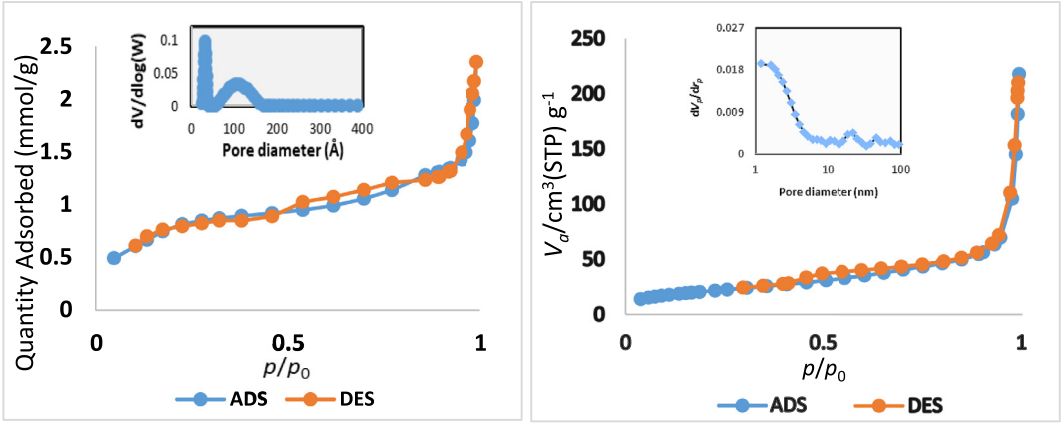

Fig. 3. The XRD pattern of Pd/HMSNs~Pyra/Pd.

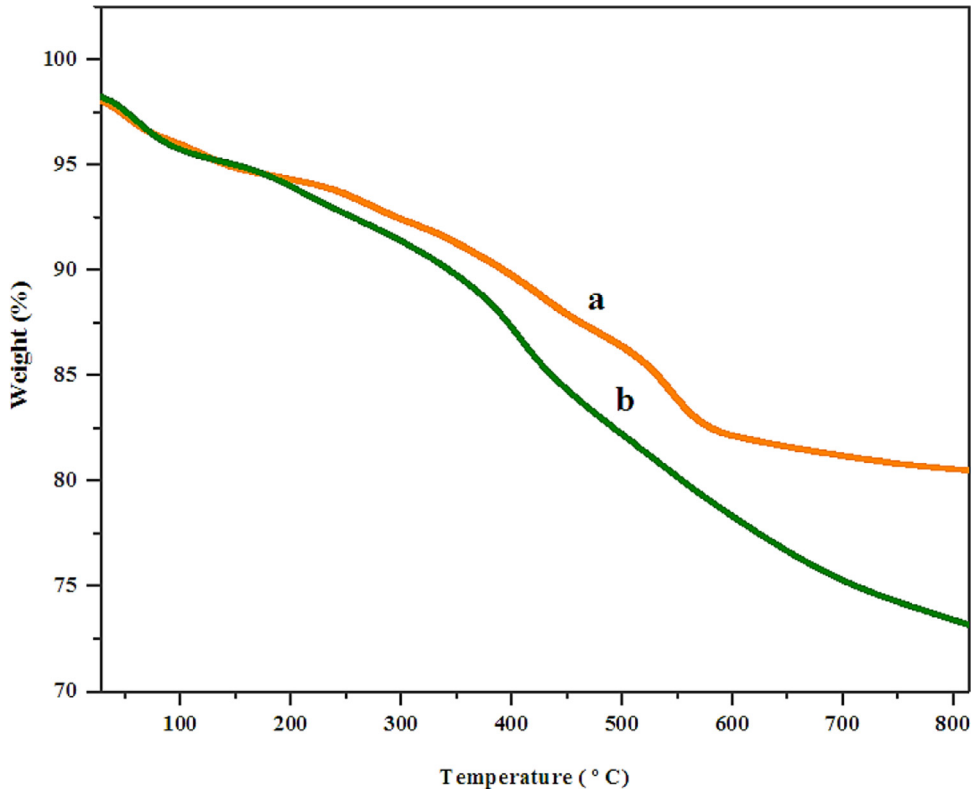

Fig. 4. EDX spectrum of Pd/HMSNs~Pyra/Pd.

Table 1
Optimization of the reaction conditions[a].

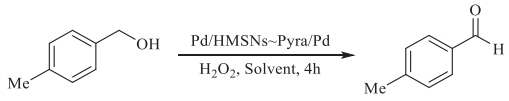

Entry	Catalyst (g, mmol%)	Solvent	H_2O_2 (equiv.)	Temperature (°C)	Yield (%)[b]
1	0.02, 3.06	H_2O	3	r.t.	trace
2	0.02, 3.06	Dichloromethane	3	r.t.	trace
3	0.02, 3.06	Toluene	3	r.t.	trace
4	0.02, 3.06	Acetonitrile	3	r.t.	65
5	0.02, 3.06	Ethanol	3	r.t.	70
6	0.02, 3.06	H_2O/Ethanol	3	r.t.	73
7	0.02, 3.06	Ethanol	3	60	80
8	0.02, 3.06	Ethanol	3	70	76
9	0.01, 1.53	Ethanol	2	60	50
10	0.03, 4.59	Ethanol	4	60	80
11	0.04, 6.12	Ethanol	5	60	82
12[c]	0.02, 3.06	Ethanol	-	60	45

[a]Reaction conditions: benzyl alcohol (1 mmol), catalyst, H_2O_2, solvent (3 mL), under air atmosphere, 4h
[b]GC yield
[c]Under air atmosphere

at ~200 °C and continued until ~800 °C, associated with the decomposition of the Pyrazolone-based ligand and organic chains of CPTES. The organic species decomposed completely at temperatures higher than 700 °C, and the residual weights of HMSNs are ~82% for HMSNs~Cl and ~72% for HMSNs~Pyra. In other words, the results demonstrate percentages of ~20% for organic fragments on the surface of HMSNs~Pyra.

2.2. Catalytic activity of Pd/HMSNs~Pyr/Pd in the selective oxidation of benzyl alcohols

The selective oxidation of benzyl alcohols was performed to evaluate the catalytic activity of the Pd/HMSNs~Pyra/Pd catalyst. To optimize the reaction conditions such as solvent, temperature, the amounts of catalyst and H_2O_2, experiments were performed for the oxidation of 4-methylbenzyl alcohol as a model reaction (Table 1). Initially, we compared the reaction rate in different solvents, such as water, dichloromethane, toluene, acetonitrile, ethanol, and a mixture of water and ethanol (1/1), using identical amounts of Pd/HMSNs~Pyra/Pd (0.02 g, 3.06 mmol%) and H_2O_2 (3 equiv.) for 4 h at room temperature (entries 1–6, Table 1). The results showed no significant product in water, dichloromethane, and toluene solvents. The desired product was obtained in ethanol; thus, ethanol was chosen as the best solvent. Next, the reaction was carried out in ethanol with increasing temperature, which resulted in 80% yield of the product at 60 °C (entry 7, Table 1). In the case of entry 8, by increasing the temperature to 70 °C, no sig-

nificant increase was observed in the yield. The model reaction in ethanol at 60 °C was also investigated using different amounts of catalyst and H_2O_2 (entries 9,10, and 11, Table 1). It was observed that when the amounts of the catalyst and H_2O_2 were increased, no significant increase was obtained in the yield of the reaction (entries 10 and 11, Table 1). The effect of oxidant on the reaction was also investigated. The result showed that the reaction afforded high yield in the presence of hydrogen peroxide instead of air (entry 12, Table 1). The high conversion of this reaction is related to the high activity of H_2O_2 oxidant. Therefore, it was concluded that the best results were obtained when the reaction was carried out at 60 °C in ethanol using 3.0 equivalent of H_2O_2 and 0.02 g (3.06 mmol%) of Pd/HMSNs~Pyra/Pd (entry 7, Table 1).

In the optimized conditions, the Pd/HMSNs~Pyra/Pd catalyst was explored for the oxidation of a various benzylic alcohol derivatives (Table 2). Benzyl alcohols with electron-donating groups showed a higher yield than the compounds with electron-withdrawing groups. In all reactions, we observed more than

Table 2
Oxidation of benzyl alcohols using Pd/HMSNs~Pyra/Pd catalyst[a,b].

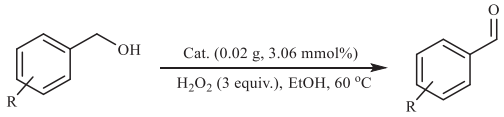

Entry	Substrate	Product	Time (h)	Conversion (%)[b]	TOF (h^{-1})
1	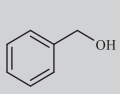	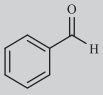	4	70	5.71
2	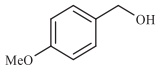	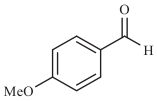	3	82	8.93
3	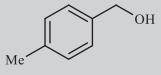	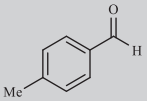	4	80	6.54
4	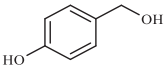	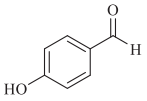	3	83	9.04
5	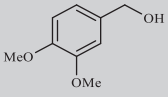	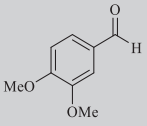	3	85	9.26
6	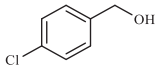	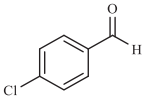	5	68	4.44
7	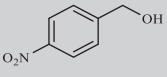	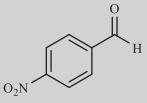	6	68	3.70
8	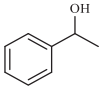		2	92	15.03
9	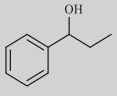	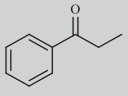	3	90	9.80
10	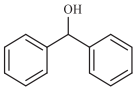	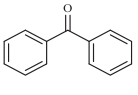	2	95	15.52

(*continued on next page*)

Table 2 (*continued*)

11	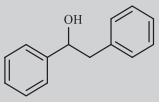	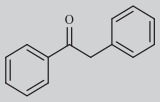	2	92	15.03
12			3	90	9.80
13			4	86	7.02
14	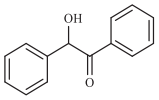	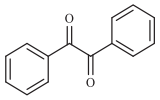	3	94	10.24
15	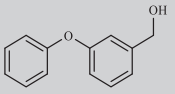	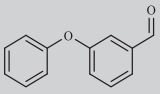	4	83	6.78

[a]Reactions conditions: alcohol (1 mmol), catalyst (0.02 g, 3.06 mmol%), H_2O_2 (3 equiv.) at 60 °C, under air atmosphere in EtOH.
[b]GC analysis

Table 3
Catalytic performance of different Pd-based catalysts in oxidation of benzyl alcohols.

Catalyst	Conditions	Time (h)	Selectivity (%)	Conversion (%)
Fe_3O_4@N-C@Pd Y-S	K_2CO_3, $PhCH_3$, 90 °C, air [87]	10	99	92
Pd-Laccase@MMCF	HQ, phosphate buffer/THF, 40 °C, air [61]	18	99	99
Pd/CNTs	Xylene, 90 °C, air [37]	6	89	98
Pd/MagSBA	Solvent free, 85 °C, O_2 [88]	10	83.2	80
Pd/NOMC−0.3–750	Solvent free, 160 °C, O_2 [89]	3	85.71	24.63
Pd@PDC	H_2O, K_2CO_3, O_2, 90 °C [90]	5	99	96
This work	EtOH, H_2O_2, 60 °C	4	99	70

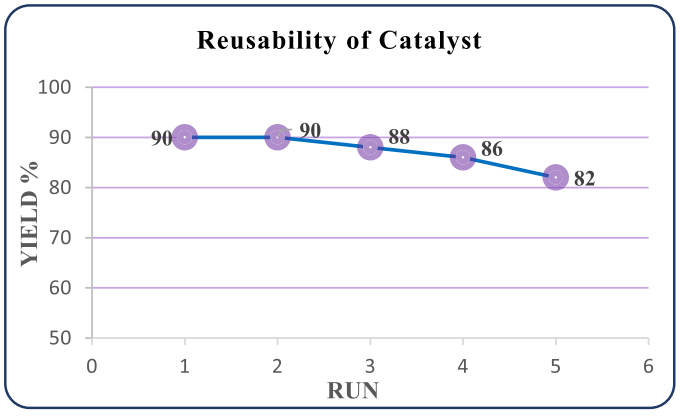

Fig. 5. N_2 adsorption/desorption isotherms and pore size distribution of (a) HMSNs~Pyra and (b) Pd/HMSNs~Pyra/Pd.

99% selectivity without any over-oxidation to benzoic acid and ester.

In addition to the catalytic activity, the reusability of heterogeneous catalysts is an important factor. To clarify this issue, we have tested the oxidation of 1-phenyl-1-propanol (Table 2, entry 9) as a model reaction, using the recycled Pd/HMSNs~Pyra/Pd catalyst. The catalyst was easily recovered by centrifugation, washed with methanol, and finally dried at 80 °C for 2 h. Then, the recovered catalyst was used in a new reaction under the same conditions. It can be seen in Fig. 7 that Pd/HMSNs~Pyra/Pd catalyst showed good

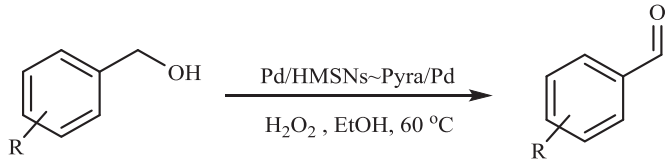

Fig. 6. TGA curves of (a) HMSNs~Cl and (b) HMSNs~Pyra.

catalytic stability after five runs without a noticeable decrease in its catalytic activity.

Table 3 shows the efficiency of the prepared catalyst compared with other reported Pd-based catalysts for the oxidation of benzyl alcohols. The current method is more straightforward, more efficient, and less time-consuming, with a lower temperature for the oxidation of benzyl alcohols.

3. Conclusion

In conclusion, we have successfully synthesized and characterized a novel heterogeneous catalyst based on palladium nanoparticles. Organo-functionalized hollow mesoporous silica nanoparticles, by exploiting both their functionalized surface and porous shell were used to support the immobilization of palladium nanoparticles. The hollow mesoporous silica nanoparticles were easily prepared by removing the Fe_3O_4 NPs as hard template and CTAB from Fe_3O_4@CTAB/SiO_2 core-shell in acidic solution. The resulting Pd/HMSNs~Pyra/Pd catalyst showed excellent selectivity

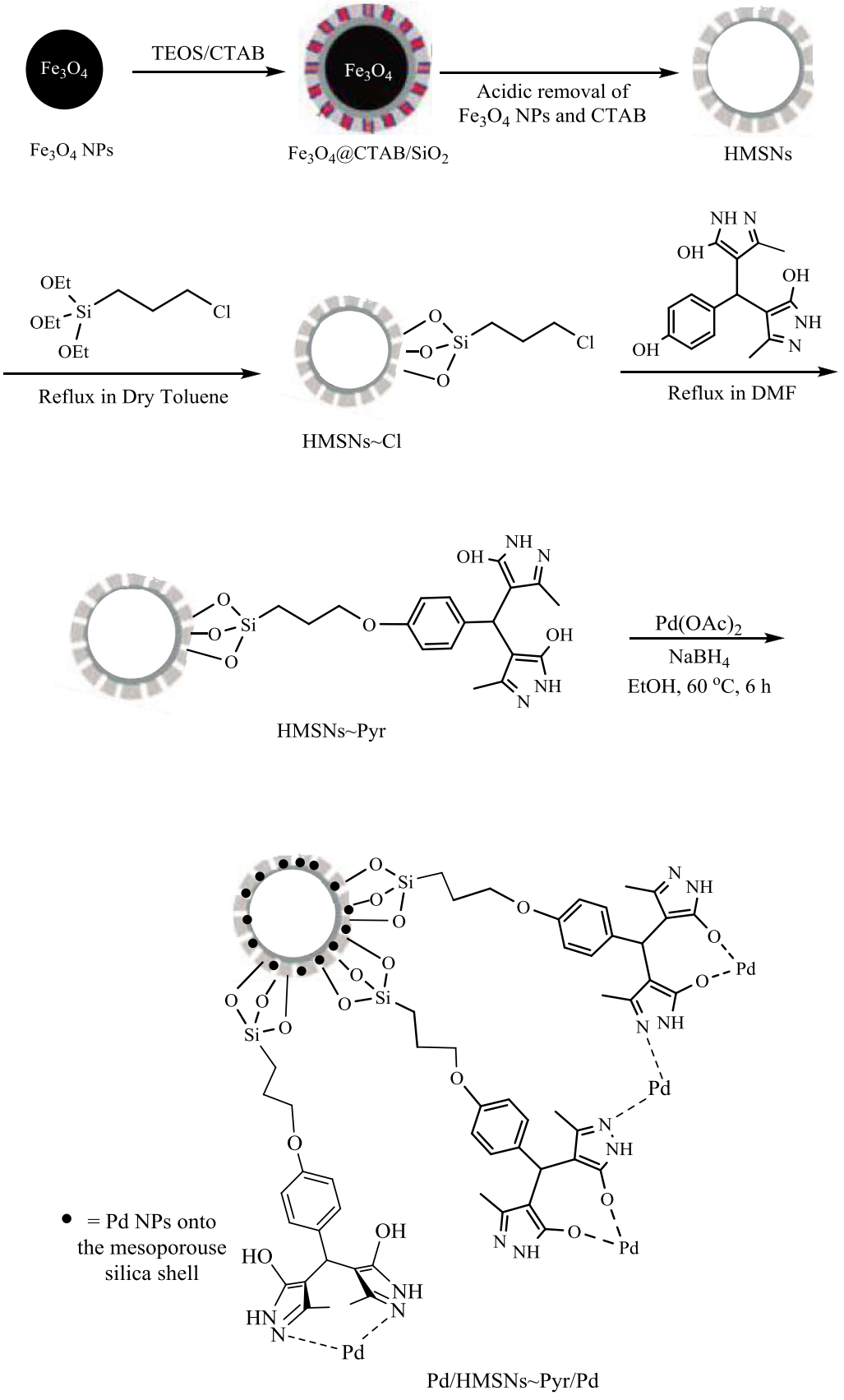

Fig. 7. Reusability of the catalyst for oxidation of 1-phenyl-1-propanol (model reaction: entry 9, Table 2).

and high catalytic activity in oxidation reactions of benzyl alcohols to the corresponding carbonyl compounds in the presence of hydrogen peroxide in ethanol as solvent at 60 °C. Easy separation, high stability, reusability, and excellent selectivity without any over oxidation are advantages of this heterogeneous catalyst. These advantages are beneficial, where an alcoholic group should be selectively oxidized to its aldehyde, especially in the total synthesis of drug molecules.

4. Experimental

4.1. General remarks

The chemicals were purchased from Fluka, SigmaAldrich, and Merck companies and were used without further purification. All reactions were monitored by TLC. Infrared spectra were recorded using a Ray Leigh Wqf510 FT-IR instrument. Transition electron microscopy (TEM) analysis was performed using a Zeiss-EM10C (Germany) operated at 100 kV V electron beam accelerating voltage. Emission scanning electron microscopy (SEM) and energy-dispersive X-ray (EDX) were performed on a TESCAN- MIRA3 operated at 26 kV with the electron gun filament: tungsten. XRD patterns were recorded using an STOE STADI-P diffractometer with monochromatic Cu-Ka radiation (wavelength = 1.54060 Å). To determine the organic content in a sample, thermogravimetric analyses were investigated using an STA PT-1000 Linseis instrument (Germany) at a heating rate of 10 °C min^{-1} under air atmosphere. The amount of Pd NPs loaded on the nanocatalyst was determined by Perkin Elmer Optima 7300D inductively coupled plasma (ICP). The specific surface area (BET method), total pore volume, and mean pore diameter (BJH method) were measured using an N_2 adsorption-desorption isotherm by using a BEISORP Mini Microtrac Bel Crop instrument.

4.2. Preparation of catalyst

4.2.1. Synthesis of silica-coated magnetite NPs (Fe_3O_4@CTAB/SiO_2 NPs)

Magnetite (Fe_3O_4) NPs were prepared according to the reported procedure (co-precipitation) [78]. Briefly, 10 mmol (2.7 g) of $FeCl_3.6H_2O$ and 5 mmol (1.0 g) of $FeCl_2.4H_2O$ were dissolved in 130 mL deionized water under nitrogen gas with vigorous stirring. Then, NH_3 (25%) was added to the solution until the pH of the solution reached 11, the orange color of the solution changed to black immediately. Stirring was continued for 1 h at 60 °C. The resultant magnetite precipitate was separated from the solution using a magnet, washed several times with deionized water and ethanol, and left to dry in the air. Subsequently, Fe_3O_4@CTAB/SiO_2 NPs were synthesized by coating a mesoporous silica layer on the surface of Fe_3O_4 NPs (sol-gel method) [79]. Typically, 0.1 g Fe_3O_4 NPs and 0.60 g CTAB were dispersed in a mixture of ethanol (60 mL) and water (100 mL) by ultrasonic treatment for 30 min. Then, 6.0 mL ammonia solution (25%) was added to the mixture, followed by the addition of TEOS solution (3.0 mL in 20 mL ethanol) slowly under stirring and left at 30 °C for 24 h. After magnetic separation, the final product (Fe_3O_4@CTAB/SiO_2 NPs) was washed with water and ethanol and dried under vacuum.

4.2.2. Preparation of hollow mesoporous silica NPs (HMSNs)

HMSNs were prepared after removing both Fe_3O_4 NPs and CTAB templates in a single step by acid treatment. Fe_3O_4@CTAB/SiO_2 NPs were dispersed in acidic ethanol (HCl, 37%) and then heated at 80 °C. After a while, the color of the solution turned from dark brown to bright yellow due to the dissolution of the Fe_3O_4 NPs [91]. The mixture was stirred continuously overnight for the complete removal of the templates. The resultant white HMSNs were separated by centrifugation, washed with ethanol, and dried in an oven at 60 °C. Finally, to ensure complete removal of CTAB and other organic components, the resulting white solid product was calcined at 550 °C for 5 h in air.

4.2.3. Preparation of modified HMSNs (HMSNs~Cl)

The chloro modified HMSNs (HMSNs~Cl) were prepared using a post-modification method with 3-chloropropyltriethoxysilane (CPTES). In brief, 0.2 g of prepared HMSNs were mixed with 10 mL of dry toluene by ultrasonic treatment, then 0.6 mL CPTES was added to the mixture. The mixture was stirred for 24 h under reflux at 110 °C. After cooling, the mixture was centrifuged and washed thoroughly twice with ethanol and distilled water to remove unreacted CPTES. The resultant HMSNs~Cl was dried under vacuum at 60 °C for 24 h.

4.2.4. Synthesis of pyrazolone-based ligand (Pyra)

A solution of hydrazine hydrate (2 mmol), ethyl acetoacetate (2 mmol), and acetic acid (2 equiv.) in water/EtOH (2:1) was stirred at 70 °C. After 15 min, 4-hydroxybenzaldehyde (1 mmol) was added, and the mixture was stirred at 70 °C for 12 h. After completion of the reaction, as indicated by TLC, the precipitated solid was filtered and washed with the mixture of water/ethanol (1:1) to obtain the 4,4′-((4-hydroxyphenyl)methylene)bis(3-methyl-1H-pyrazol-5-ol) as a pure white powder in 90% yield. Mp 267–270 °C. IR (KBr) (υ_{max}/cm^{-1}): 3403, 2924, 1709, 1595, 1483. MS, (*m/z*): 301(*M*+1), 299, 267, 241, 203, 186, 115. ^{1}H NMR (300 MHz, DMSO-d_6): δ_H (ppm) 2.12 (6 H, s, 2 CH_3), 4.78 (1H, s, CH), 5.54 (2NH, and 3OH exchanged with water of DMSO-d_6), 6.67 (2H, *d*, $^3J_{HH}$ = 8.4 Hz, HAr), 7.00 (2H, *d*, $^3J_{HH}$ = 8.4 Hz, HAr). ^{13}C NMR (75 MHz, DMSO-d_6): δ_C (ppm)10.3 (CH_3), 31.9 (CH), 104.8, 114.6, 128.3, 133.3, 140.1, 155.1, 161.1(C-Ar). Anal. Calcd. for $C_{15}H_{16}N_4O_3$: C, 59.99; H, 5.37; N, 18.66. Found: C, 59.96; H, 5.33; N, 18.71.

4.2.5. Functionalization of the modified HMSNs (HMSNs~Pyra)

The 4,4′-((4-hydroxyphenyl)methylene)bis(3-methyl-1H-pyrazol-5-ol) (0.3 g, 1 mmol) was added into a suspension of HMSNs~Cl (0.2 g) in dry DMF (50 mL). The reaction mixture was refluxed at 140 °C in an oil bath for 24 h. The resulting precipitate was centrifuged and washed with DMF, followed by distilled water, ethanol, and acetone. Finally, the HMSNs~Pyra was dried at 100 °C for 24 h.

4.2.6. Preparation of Pd/HMSNs~Pyra/Pd NPs

To a stirred solution of $Pd(OAc)_2$ (0.134 g, 0.6 mmol) in water (30 mL) was added HMSNs~Pyra (0.3 g). The mixture was stirred for 0.5 h to form a brown mixture, and then a solution of $NaBH_4$ (0.11 g, 3 mmol) in EtOH (10 mL) was added. The color of the mixture immediately turned to black. After stirring for 6 h at 60 °C, the product was obtained by centrifugation, washed with EtOH twice, and dried at 70 °C overnight to give dark gray Pd/HMSNs~Pyra/Pd nanocatalyst. The amount of Pd loaded on the 0.1 g of Pd/HMSNs~Pyra/Pd NPs was 0.153 mmol (16.27 wt%), as detected by ICP.

4.3. General procedure for oxidation of benzyl alcohols using Pd/HMSNs~Pyra/Pd nanocatalyst

To a mixture of benzylic alcohol (1.0 mmol) and Pd/HMSNs~Pyra/Pd nanocatalyst (0.02 g, 3.06 mmol%) in ethanol (5 mL), H_2O_2 (3 equiv.) was added dropwise under stirring at room temperature. The reaction was continuously stirred at 50 °C for an appropriate reaction time. After completing the reaction, as indicated by TLC, the reaction mixture was centrifuged, and the nanocatalyst was separated. Then, the remaining solution was analyzed by the GC-MS method to obtain the yield and selectivity

of the reaction. The results showed >99% selectivity to aldehyde or ketone without any over oxidation to benzoic acid and ester. The results of GC-mass analysis for this oxidation reaction can be found in the supporting information section.

Declaration of Competing Interest

The authors declare that they have no known competing financial interests or personal relationships that could have appeared to influence the work reported in this paper.

Acknowledgments

The authors acknowledge the Razi University Research Council for support of this work.

References

[1] E. Nikolla, Y. Roman-Leshkov, M. Moliner, M.E. Davis, One-pot" synthesis of 5-(hydroxymethyl)furfural from carbohydrates using tin-beta zeolite, ACS Catal. 1 (2011) 408–410, doi:10.1021/cs2000544.
[2] P. Barbaro, F. Liguori, Ion exchange resins: catalyst recovery and recycle, Chem. Rev. 109 (2009) 515–529, doi:10.1021/cr800404j.
[3] D.C. Sherrington, A.P. Kybett, Supported Catalysts and Their Applications, RSC, Cambridge, UK, 2001.
[4] P. Munnik, P.E. de Jongh, K.P. de Jong, Recent developments in the synthesis of supported catalysts, Chem. Rev. 115 (2015) 6687–6718, doi:10.1021/cr500486u.
[5] J.G. Wang, F. Li, H.J. Zhou, P.C. Sun, D.T. Ding, T.H. Chen, Silica hollow spheres with ordered and radially oriented amino-functionalized mesochannels, Chem. Mater. 21 (2009) 612–620, doi:10.1021/cm803124a.
[6] M. Jafarzadeh, R. Adnan, M.K.N. Mazlan, Thermal stability and optical property of ormocers (organically modified ceramics) nanoparticles produced from copolymerization between amino-silanes and tetraethoxysilane, J. Non. Cryst. Solids 385 (2012) 2981–2987, doi:10.1016/j.jnoncrysol.2012.07.028.
[7] Z.S. Qureshi, P.B. Sarawade, M. Albert, V. D'Elia, M.N. Hedhili, K. Köhler, J-M Basset, Palladium nanoparticles supported on fibrous-structured silica nanospheres (KCC-1): an efficient and selective catalyst for the transfer hydrogenation of alkenes, ChemCatChem 7 (2015) 635–642, doi:10.1002/cctc.201402781.
[8] W. Yang, X. Xiao, R. Lu, H. Xie, M. Xu, M. Liu, Q. Sun, M. Tian, Synthesis of novel TiO_2/BiOCl@HHSS composites and its photocatalytic activity enhancement under simulated sunlight, RSC Adv. 6 (2016) 101242–101249, doi:10.1039/C6RA11904B.
[9] W. Zhu, Z. Chen, Y. Pan, R. Dai, Y. Wu, Z. Zhuang, D. Wang, Q. Peng, C. Chen, Y. Li, Functionalization of hollow nanomaterials for catalytic applications: nanoreactor construction, Adv. Mater. 31 (2018) e1800426, doi:10.1002/adma.201800426.
[10] J. Zhang, Y. Cao, C-A. Wang, R. Ran, Design and preparation of MnO_2/CeO_2–MnO_2 double-shelled binary oxide hollow spheres and their application in CO oxidation, ACS Appl. Mater. Interfaces 8 (2016) 8670–8677, doi:10.1021/acsami.6b00002.
[11] M. Gao, J. Zeng, K. Liang, D. Zhao, B. Kong, Interfacial assembly of mesoporous silica-based optical heterostructures for sensing applications, Adv. Funct. Mater. 30 (2020) 1906950, doi:10.1002/adfm.201906950.
[12] K. Yang, Y. Liu, Y. Liu, Q. Zhang, C. Kong, C. Yi, Z. Zhou, Z. Wang, G. Zhang, Y. Zhang, N.M. Khashab, X. Chen, Z. Nie, Cooperative assembly of magneto-nanovesicles with tunable wall thickness and permeability for MRI-guided drug delivery, J. Am. Chem. Soc. 140 (2018) 4666–4677, doi:10.1021/jacs.8b00884.
[13] Y.P. Zhu, T.Y. Ma, M. Jaroniec, S.Z. Qiao, Self-templating synthesis of hollow Co_3O_4 microtube arrays for highly efficient water electrolysis, Angew. Chem. Int. Ed. 56 (2017) 1324–1328, doi:10.1002/anie.201610413.
[14] J. Wang, Y. Cui, D. Wang, Design of hollow nanostructures for energy storage, conversion and production, Adv. Mater. 31 (2018) 1801993, doi:10.1002/adma.201801993.
[15] Y. Chen, H.R. Chen, J.L. Shi, Construction of homogenous/heterogeneous hollow mesoporous silica nanostructures by silica-etching chemistry: principles, synthesis, and applications, Acc. Chem. Res. 47 (2014) 125–137, doi:10.1021/ar400091e.
[16] Z. Cai, Z. Wang, J. Kim, Y. Yamauchi, Hollow functional materials derived from metal–organic frameworks: synthetic strategies, conversion mechanisms, and electrochemical applications, Adv. Mater. 31 (2019) 1804903, doi:10.1002/adma.201804903.
[17] N. Ezzati, A.R. Mahjoub, A. Abolhosseini Shahrnoy, Z. Syrgiannis, Amino acid-functionalized hollow mesoporous silica nanospheres as efficient biocompatible drug carriers for anticancer applications, Int. J. Pharm. 572 (2019) 118709, doi:10.1016/j.ijpharm.2019.118709.
[18] Z. Chen, L. Wan, Y. Yuan, Y. Kuang, X. Xu, T. Liao, J. Liu, Z-Q. Xu, B. Jiang, C. Li, pH/GSH-Dual-sensitive hollow mesoporous silica nanoparticle-based drug delivery system for targeted cancer therapy, ACS Biomater. Sci. Eng. 6 (2020) 3375–3387, doi:10.1021/acsbiomaterials.0c00073.
[19] S.P.H. Moghaddam, M. Yazdimamaghani, H. Ghandehari, Glutathione-sensitive hollow mesoporous silica nanoparticles for controlled drug delivery, J. Control Release 282 (2018) 62–75, doi:10.1016/j.jconrel.2018.04.032.
[20] Y. Wu, J. Lu, Y. Mao, T. Jiang, Q. Zhao, S. Wang, Composite phospholipid-coated hollow mesoporous silica nanoplatform with multi-stimuli responsiveness for combined chemo-photothermal therapy, J. Mater Sci. 55 (2020) 5230–5246, doi:10.1007/s10853-019-04314-w.
[21] F. Hoffmann, M. Cornelius, J. Morell, M. Froba, Silica-based mesoporous organic–inorganic hybrid materials, Angew. Chem. Int. Ed. Engl. 45 (2006) 3216–3251, doi:10.1002/anie.200503075.
[22] M. Nikoorazm, A. Ghorbani-Choghamarani, N. Noori, B. Tahmasbi, Palladium 2-mercapto-N-propylacetamide complex anchored onto MCM-41 as efficient and reusable nanocatalyst for Suzuki, Stille and Heck reactions and amination of aryl halides, Appl. Organometal. Chem. 30 (2016) 843–851, doi:10.1002/aoc.3512.
[23] M. Xie, X. Dai, S. Meng, X. Fu, S. Chen, Selective oxidation of aromatic alcohols to corresponding aromatic aldehydes using In_2S_3 microsphere catalyst under visible light irradiation, Chem. Eng. J. 245 (2014) 107–116, doi:10.1016/j.cej.2014.02.029.
[24] A.L. Cánepa, V.R. Elías, V.M. Vaschetti, E.V. Sabre, G.A. Eimer, S.G. Casuscelli, Selective oxidation of benzyl alcohol through eco-friendly processes using mesoporous V-MCM-41, Fe-MCM-41 and Co-MCM-41 materials, Appl. Catal. A 545 (2017) 72–78, doi:10.1016/j.apcata.2017.07.039.
[25] L.M.D.R.D. Martins, S.A.C. Carabineiro, J. Wang, B.G.M. Rocha, F.J. Maldonado-Hódar, A.J.L.D.O. Pombeiro, Supported gold nanoparticles as reusable catalysts for oxidation reactions of industrial significance, ChemCatChem 9 (2017) 1211–1221, doi:10.1002/cctc.201601442.
[26] S.M. Sarathy, P. Oßwald, N. Hansen, K. Kohse-Höinghaus, Alcohol combustion chemistry, Prog. Energy Combust. Sci. 44 (2014) 40–102, doi:10.1016/j.pecs.2014.04.003.
[27] Y. Li, Y. Gao, C. Yang, A facile and efficient synthesis of polystyrene/gold–platinum composite particles and their application for aerobic oxidation of alcohols in water, Chem. Commun. 51 (2015) 7721–7724, doi:10.1039/C5CC01053E.
[28] N. Jamwal, M. Gupta, S. Paul, Hydroxyapatite-supported palladium(0) as a highly efficient catalyst for the Suzuki coupling and aerobic oxidation of benzyl alcohols in water, Green Chem 10 (2008) 999–1003, doi:10.1039/B802135J.
[29] S.F.J. Hackett, R.M. Brydson, M.H. Gass, I. Harvey, A.D. Newman, K. Wilson, A.F. Lee, High-activity, single-site mesoporous Pd/Al_2O_3 catalysts for selective aerobic oxidation of allylic alcohols, Angew. Chem. 119 (2007) 8747–8750, doi:10.1002/ange.200702534.
[30] C.P. Vinod, K. Wilson, A.F. Lee, Recent advances in the heterogeneously catalysed aerobic selective oxidation of alcohols, J. Chem. Technol. Biotechnol. 86 (2010) 161–171, doi:10.1002/jctb.2504.
[31] A. Díaz-Rodríguez, L. Martínez-Montero, I. Lavandera, V. Gotor, V. Gotor-Fernández, Laccase/2,2,6,6-tetramethylpiperidinoxyl radical (TEMPO): An efficient catalytic system for selective oxidations of primary hydroxy and amino groups in aqueous and biphasic media, Adv. Synth. Catal. 356 (2014) 2126-2126, doi:10.1002/adsc.201400589.
[32] T. Mallat, A. Baiker, Oxidation of alcohols with molecular oxygen on solid catalysts, Chem. Rev. 104 (2004) 3037–3058, doi:10.1021/cr0200116.
[33] S.E. Davis, M.S. Ide, R.J. Davis, Selective oxidation of alcohols and aldehydes over supported metal nanoparticles, Green Chem. 15 (2013) 17–45, doi:10.1039/C2GC36441G.
[34] Y. Sun, X. Li, J. Wang, W. Ning, J. Fu, X. Lu, Z. Hou, Carbon film encapsulated Pt NPs for selective oxidation of alcohols in acidic aqueous solution, Appl. Catal. B 218 (2017) 538–544, doi:10.1016/j.apcatb.2017.06.086.
[35] D. Ferri, C. Mondelli, F. Krumeich, A. Baiker, Discrimination of active palladium sites in catalytic liquid-phase oxidation of benzyl alcohol, J. Phys. Chem. B 110 (2006) 22982–22986, doi:10.1021/jp065779z.
[36] S. Gowrisankar, H. Neumann, D. Gordes, K. Thurow, H. Jiao, M. Beller, A convenient and selective palladium-catalyzed aerobic oxidation of alcohols, Chem. Eur. J. 19 (2013) 15979–15984, doi:10.1002/chem.201302526.
[37] V.M. Shinde, E. Skupien, M. Makkee, Synthesis of highly dispersed Pd nanoparticles supported on multi-walled carbon nanotubes and their excellent catalytic performance for oxidation of benzyl alcohol, Catal. Sci. Technol. 5 (2015) 4144–4153, doi:10.1039/C5CY00563A.
[38] H. Yamaoka, N. Moriya, M. Ikunaka, A practical $RuCl_3$-catalyzed oxidation using trichloroisocyanuric acid as a stoichiometric oxidant under mild nonacidic conditions, Org. Process Res. Dev. 8 (2004) 931–938, doi:10.1021/op049940k.
[39] I. Dobrosz-Gómez, I. Kocemba, J.M. Rynkowski, Factors influencing structure and catalytic activity of $Au/Ce1-xZrxO_2$ catalysts in CO oxidation, Appl. Catal. B Environ. 88 (2009) 83–97, doi:10.1016/j.apcatb.2008.09.028.
[40] A. Abad, P. Concepción, A. Corma, H. García, A collaborative effect between gold and a support induces the selective oxidation of alcohols, Angew. Chem. Int. Ed. 44 (2005) 4066–4069, doi:10.1002/anie.200500382.
[41] E.V. Johnston, O. Verho, M.D. Kärkäs, M. Shakeri, C.-W. Tai, P. Palmgren, K. Eriksson, S. Oscarsson, J.-E. Bäckvall, Highly dispersed palladium nanoparticles on mesocellular foam: an efficient and recyclable heterogeneous catalyst for alcohol oxidation, Chem. Eur. J. 18 (2012) 12202–12206, doi:10.1002/chem.201202157.
[42] D.I. Enache, J.K. Edwards, P. Landon, B.S. Espriu, A.F. Carley1, A.A. Herzing, M. Watanabe, C.J. Kiely, D.W. Knight, G.J. Hutchings, Solvent-free oxidation of primary alcohols to aldehydes using $Au-Pd/TiO_2$ catalysts, Science 311 (2006) 362–365, doi:10.1126/science.1120560.

[43] K. Mori, T. Hara, T. Mizugaki, K. Ebitani, K. Kaneda, Hydroxyapatite-supported palladium nanoclusters: a highly active heterogeneous catalyst for selective oxidation of alcohols by use of molecular oxygen, J. Am. Chem. Soc. 126 (2004) 10657–10666, doi:10.1021/ja0488683.

[44] B. Karimi, S. Abedi, J.H. Clark, V. Budarin, Highly efficient aerobic oxidation of alcohols using a recoverable catalyst: the role of mesoporous channels of SBA-15 in stabilizing palladium nanoparticles, Angew. Chem. Int. Ed. 45 (2006) 4776–47779, doi:10.1002/anie.200504359.

[45] B. Karimi, A. Zamani, S. Abedi, J.H. Clark, Aerobic oxidation of alcohols using various types of immobilized palladium catalyst: the synergistic role of functionalized ligands, morphology of support, and solvent in generating and stabilizing nanoparticles, Green Chem. 11 (2009) 109–119, doi:10.1039/B805824E.

[46] T. Yasu-eda, R. Se-ike, N. Ikenaga, T. Miyake, T. Suzuki, Palladium-loaded oxidized diamond catalysis for the selective oxidation of alcohols, J. Mol. Catal. A Chem. 306 (2009) 136–142, doi:10.1016/j.molcata.2009.02.039.

[47] T. Harada, S. Ikeda, F. Hashimoto, T. Sakata, K. Ikeue, T. Torimoto, M. Matsumura, Catalytic activity and regeneration property of a Pd nanoparticle encapsulated in a hollow porous carbon sphere for aerobic alcohol oxidation, Langmuir 26 (2010) 17720–17725, doi:10.1021/la102824s.

[48] C.E. Chan-Thaw, A. Villa, L. Prati, A. Thomas, Triazine-based polymers as nanostructured supports for the liquid-phase oxidation of alcohols, Chem. A Eur. J. 17 (2011) 1052–1057, doi:10.1002/chem.201000675.

[49] X. Wang, G. Wu, N. Guan, L. Li, Supported Pd catalysts for solvent-free benzyl alcohol selective oxidation: effects of calcination pretreatments and reconstruction of Pd sites, Appl. Catal. B 115-116 (2012) 7–15, doi:10.1016/j.apcatb.2011.12.011.

[50] S. Gowrisankar, H. Neumann, D. Gordes, K. Thurow, H. Jiao, M. Beller, A convenient and selective palladium-catalyzed aerobic oxidation of alcohols, Chem. A Eur. J. 19 (2013) 15979–15984, doi:10.1002/chem.201302526.

[51] M.M. Dell'Anna, M. Mali, P. Mastrorilli, P. Cotugno, A. Monopoli, Oxidation of benzyl alcohols to aldehydes and ketones under air in water using a polymer supported palladium catalyst, J. Mol. Catal. A 386 (2014) 114–119, doi:10.1016/j.molcata.2014.02.001.

[52] C.E. Chan-Thaw, A. Savara, A. Villa, Selective benzyl alcohol oxidation over Pd catalysts, Catalysts 8 (2018) 431, doi:10.3390/catal8100431.

[53] L. Chen, J. Yan, Z. Tong, S. Yu, J. Tang, B. Ou, L. Yue, L. Tian, Nanofiber-like mesoporous alumina supported palladium nanoparticles as a highly active catalyst for base-free oxidation of benzyl alcohol, Micropor. Mesopor. Mat. 266 (2018) 126–131, doi:10.1016/j.micromeso.2018.02.037.

[54] H. Zheng, Z.H. Wei, X.Q. Hu, J. Xu, B. Xue, Atmospheric selective oxidation of benzyl alcohol catalyzed by Pd nanoparticles supported on CeO_2 with various morphologies, ChemistrySelect 4 (2019) 5470–5475, doi:10.1002/slct.201900757.

[55] W. Zhu, Z. Chen, Y. Pan, R. Dai, Y. Wu, Z. Zhuang, D. Wang, Q. Peng, C. Chen, Y. Li, Functionalization of hollow nanomaterials for catalytic applications: nanoreactor construction, Adv. Mater. 31 (2019) 1800426, doi:10.1002/adma.201800426.

[56] C.Y. Ma, B.J. Dou, J.J. Li, J. Cheng, Q. Hu, Z.P. Hao, S.Z. Qiao, Catalytic oxidation of benzyl alcohol on Au or Au–Pd nanoparticles confined in mesoporous silica, Appl. Catal. B Environ. 92 (2009) 202–208, doi:10.1016/j.apcatb.2009.07.007.

[57] J. Liu, H.Q. Yang, F. Kleitz, Z.G. Chen, T.Y. Yang, E. Strounina, G.Q. Lu, S.Z. Qiao, Yolk–shell hybrid materials with a periodic mesoporous organosilica shell: ideal nanoreactors for selective alcohol oxidation, Adv. Funct. Mater. 22 (2012) 591–599, doi:10.1002/adfm.201101900.

[58] X. Du, J. He, Amino-functionalized silicananoparticles with center-radially hierarchical mesopores as ideal catalyst carriers, Nanoscale 4 (2012) 852–859, doi:10.1039/C1NR11504A.

[59] C.M.A. Parlett, D.W. Bruce, N.S. Hondow, M.A. Newton, A.F. Lee, K. Wilson, Mesoporous silicas as versatile supports to tune the palladium-catalyzed selective aerobic oxidation of allylic alcohols, ChemCatChem 5 (2013) 939–950, doi:10.1002/cctc.201200301.

[60] C.H. Tsai, M. Xu, P. Kunal, B.G. Trewyn, Aerobic oxidative esterification of primary alcohols over Pd-Au bimetallic catalysts supported on mesoporous silica nanoparticles, Catal. Today 306 (2018) 81–88, doi:10.1016/j.cattod.2017.01.046.

[61] Z. Shokri, N. Azimi, S. Moradi, A. Rostami, A novel magnetically separable laccase-mediator catalyst system for the aerobic oxidation of alcohols and 2-substituted-2,3-dihydroquinazolin-4(1H)-ones under mild conditions, Appl. Organometal. Chem. 34 (2020) e5899, doi:10.1002/aoc.5899.

[62] J. Lyu, L. Niu, F. Shen, J. Wei, Y. Xiang, Z. Yu, G. Zhang, C. Ding, Y. Huang, X. Li, *In situ* hydrogen peroxide production for selective oxidation of benzyl alcohol over a Pd@hierarchical titanium silicalite catalyst, ACS Omega 5 (2020) 16865–16874, doi:10.1021/acsomega.0c02065.

[63] N. Raman, A. Kulandaisamy, A. Shunmugasundaram, K. Jeyasubramanian, Synthesis, spectral, redox and antimicrobial activities of Schiff base complexes derived from 1-phenyl-2,3-dimethyl-4-aminopyrazol-5-one and acetoacetanilide, Trans. Met. Chem. 26 (2001) 131–135, doi:10.1023/A:1007100815918.

[64] B.A. Uzoukwu, P.U. Adiukwu, S.S. Al-Juaid, P.B. Hitchcock, J.D. Smith, Pyrazolonato complexes of lead. Crystal structures of bis(1-phenyl-3-methyl-4-acetyl pyrazolonato)lead(II) and bis(1-phenyl-3-methyl-4-butanoylpyrazolonato)lead(II), Inorg. Chim. Acta 250 (1996) 173–176, doi:10.1016/S0020-1693(96)05224-3.

[65] V.A. Joseph, J.H. Pandya, R.N. Jadeja, Syntheses, crystal structure and biological evaluation of Schiff bases and copper complexes derived from 4-formylpyrazolone, J. Mol. Struct. 1081 (2015) 443–448, doi:10.1016/j.molstruc.2014.10.056.

[66] Z.Y. Yang, R.D. Yang, F.S. Li, K.B. Yu, Crystal structure and antitumor activity of some rare earth metal complexes with Schiff base, Polyhedron 19 (2000) 2599–2604, doi:10.1016/S0277-5387(00)00562-3.

[67] W.F. Yang, S.G. Yuan, Y.B. Xu, Y.H. Xiao, K.M. Fang, Extraction of thorium traces from hydrochloric acid media by 1-phenyl-3-methyl-4-benzoyl-pyrazolone-5, J. Radioanal. Nucl. Chem. 256 (2003) 149–152, doi:10.1023/a:1023324714875.

[68] P. Chiba, W. Holzer, M. Landau, G. Bechmann, K. Lorenz, B. Plagens, M. Hitzler, E. Richter, G. Ecker, Substituted 4-acylpyrazoles and 4-acylpyrazolones: synthesis and multidrug resistance-modulating activity, J. Med. Chem. 41 (1998) 4001–4011, doi:10.1021/jm980121y.

[69] A.K. El-Sawaf, D.X. West, Synthesis, magnetic and spectral studies of nickel(II) and zinc(II) complexes of 4-formylantipyrine N(4)-substituted thiosemicarbazones, Trans. Met. Chem. 23 (1998) 417–421, doi:10.1023/A:1006996731782.

[70] N. Kalarani, S. Sangeetha, P. Kamalakannan, D. Venkappayya, Synthesis of 4-dicyclohexylaminomethyl antipyrine and its metal complexes: spectral characterization and evaluation of thermodynamic parameters, Russ. J. Coord. Chem. 29 (2003) 845–851, doi:10.1023/B:RUCO.0000008396.57645.7d.

[71] E.A. Bakr, G.B. Al-Hefnawy, M.K. Awad, H.H. Abd-Elatty, M.S. Youssef, New Ni(II), Pd(II) and Pt(II) complexes coordinated to azo pyrazolone ligand with a potent anti-tumor activity: synthesis, characterization, DFT and DNA cleavage studies, Appl. Organomet. Chem. 32 (2018) e4104, doi:10.1002/aoc.4104.

[72] Y. Zhang, Y. Li, G. Xu, J. Li, H. Luo, J. Li, L. Zhang, D. Jia, Synthesis, crystal structure, DNA/bovine serum albumin binding and antitumor activity of two transition metal complexes with 4-acylpyrazolone derivative, Appl. Organometal. Chem. 33 (2019) e4668, doi:10.1002/aoc.4668.

[73] S. Sunitha, K.K. Aravindakshan, Synthesis, characterisation and antimicrobial studies on transition metal complexes of methylphenyl-4-[phenyl (phenylhydrazono) methyl]-3-pyrazolone, Int. J. Pharm. Biomed. Sci. 3 (2013) 140–150.

[74] R. Jayarajan, G. Vasuki, P.S. Rao, Synthesis and antimicrobial studies of tridentate Schiff base ligands with pyrazolone moiety and their metal complexes, Org. Chem. Int. 2010 (2010) 648589–648596, doi:10.1155/2010/648589.

[75] D. Liu, X. Zhang, L. Zhu, J. Wu, X. Lü, Alternating ring-opening copolymerization of styrene oxide and maleic anhydride using asymmetrical bis-Schiff-base metal(III) catalysts, Catal. Sci. Technol. 5 (2015) 562–571, doi:10.1039/C4CY01064G.

[76] D.F. Liu, L.Y. Wu, W.X. Feng, X.M. Zhang, J. Wu, L.Q. Zhu, D. Di Fan, X.Q. Lü, Q. Shi, Ring-opening copolymerization of CHO and MA catalyzed by mononuclear $[Zn(L^2)(H_2O)]$ or trinuclear $[Zn_3(L^2)_2(OAc)_2]$ complex based on the asymmetrical bis-Schiff-base ligand precursor, J. Mol. Catal. A Chem. 382 (2014) 136–145, doi:10.1016/j.molcata.2013.11.002.

[77] C.K. Modi, B.G. Gade, J.A. Chudasama, D.K. Parmar, H.D. Nakum, A.L. Patel, Synthesis, spectral investigation and catalytic aspects of entrapped VO(IV) and Cu(II) complexes into the supercages of Zeolite-Y, Spectrochim. Acta Part A Mol. Biomol. Spectrosc. 140 (2015) 174–184, doi:10.1016/j.saa.2014.12.028.

[78] L. Chen, Z. Xu, H. Dai, S. Zhang, Facile synthesis and magnetic properties of monodisperse Fe_3O_4/silica nanocomposite microspheres with embedded structures via a direct solution-based route, J. Alloy. Compd. 497 (2010) 221–227, doi:10.1016/j.jallcom.2010.03.016.

[79] I.A. Rahman, V. Padavettan, Synthesis of silica nanoparticles by sol-gel: size-dependent properties, surface modification, and applications in silica-polymer nanocomposites, J. Nanomater. 8 (2012) 1, doi:10.1155/2012/132424.

[80] E. Soleimania, S. Ghorbani, M. Taran, A. Sarvary, Synthesis of 4,4′-(arylmethylene)bis(3-methyl-1H-pyrazol-5-ol) derivatives in water, C. R. Chim. 15 (2012) 955–961, doi:10.1016/j.crci.2012.07.003.

[81] V. Nairi, L. Medda, M. Monduzzi, A. Salis, Adsorption and release of ampicillin antibiotic from ordered mesoporous silica, J. Colloid Interface Sci. 497 (2017) 217–225, doi:10.1016/j.jcis.2017.03.021.

[82] M. Ghazvini, A. Abolhosseini Shahrnoy, Efficient degradation of methylene blue by Co(II) complexes constrained to the hall of mesoporous silica decorated by Pt nanoparticles, Mater. Lett. 259 (2020) 126776, doi:10.1016/j.matlet.2019.126776.

[83] S. Rostamnia, E. Doustkhah, B. Zeynizadeh, Cationic modification of SBA-15 pore walls for Pd supporting: Pd@SBA-15/ILDABCO as a catalyst for Suzuki coupling in water medium, Microporous Mesoporous Mater. 222 (2016) 87–93, doi:10.1016/j.micromeso.2015.09.045.

[84] Q.C. Do, D.G. Kim, S.O. Ko, Nonsacrificial template synthesis of magnetic-based yolk–shell nanostructures for the removal of acetaminophen in Fenton-like systems, ACS Appl. Mater. Interfaces 9 (2017) 28508–28518, doi:10.1021/acsami.7b07658.

[85] U. Yilmaz, H. Kucukbay, S.T. Celikesir, M. Akkurt, O. Buyukgungor, Synthesis of novel benzimidazole salts and microwave-assisted catalytic activity of *in situ* generated Pd nanoparticles from a catalyst system consisting of benzimidazol salt, $Pd(OAc)_2$, and base in a Suzuki-Miyaura reaction, Turk. J. Chem. 37 (2013) 721–733, doi:10.3906/kim-1207-18.

[86] F. Durap, O. Metin, M. Aydemir, S. Ozkar, New route to synthesis of PVP-stabilized palladium(0) nanoclusters and their enhanced catalytic activity in Heck and Suzuki cross-coupling reactions, Appl. Organometal. Chem. 24 (2009) 498–503, doi:10.1002/aoc.1555.

[87] S.K. Movahed, N. Farajinia Lehi, M. Dabiri, Palladium nanoparticles supported on core-shell and yolk-shell Fe_3O_4@nitrogen doped carbon cubes as a highly efficient, magnetically separable catalyst for the reduction of nitroarenes and the oxidation of alcohols, J. Catal. 364 (2018) 69–79, doi:10.1016/j.jcat.2018.05.003.

[88] Y. Li, J. Huang, X. Hu, F.L. Lam, W. Wang, R. Luque, Heterogeneous Pd catalyst for mild solvent-free oxidation of benzyl alcohol, J. Mol. Catal. A Chem. 425 (2016) 61–67, doi:10.1016/j.molcata.2016.09.030.

[89] H. Song, Z. Liu, H. Gai, Y. Wang, L. Qiao, C. Zhong, X. Yin, Meng Xiao, Nitrogen-dopped ordered mesoporous carbon anchored Pd nanoparticles for solvent free selective oxidation of benzyl alcohol to benzaldehyde by using O_2, Front. Chem. 7 (2019) 458, doi:10.3389/fchem.2019.00458.
[90] Q. Wang, X. Cai, Y. Liu, J. Xie, Y. Zhou, J. Wang, Pd nanoparticles encapsulated into mesoporous ionic copolymer: efficient and recyclable catalyst for the oxidation of benzyl alcohol with O_2 balloon in water, App. Catal. B Environ. 189 (2016) 242–251, doi:10.1016/j.apcatb.2016.02.067.
[91] M. Rochelle, R.M. Cornell, U. Schwertmann, The Iron Oxides: Structure, Properties, Reactions, Occurrences and Uses, 2nd Ed., Wiley-VCH, New York, 2003.